Determination of the Formation of Ladder Structure in Poly(5-amino-1-naphthol) by Resonant Raman and XPS Characterization

Elaine P. Cintra and Susana I. Córdoba de Torresi*

Instituto de Química, Universidade de São Paulo, C.P. 26077, 05513-970 São Paulo, Brazil

Nicolas Errien and Guy Louarn

Institut des Materiaux Jean Rouxel, Université de Nantes, 2 rue de la Houssiniere, B.P. 32229, 44322 Nantes Cedex 3, France

Received November 5, 2002; Revised Manuscript Received January 14, 2003

ABSTRACT: A study of different oxidation states of poly(5-amino-1-naphthol), poly(5-$NH_2$1-NAP), in aqueous acid solutions of chloridric and camphorsulfonic acid is presented. Resonant Raman spectroscopy was used as a tool for following structural changes provoked by not only the redox potential but also the anion used in the polymerization or cycling processes. The apparent chemical homogeneity of the films is questioned because the coexistence of different segments, in the polymeric chain, was observed. Raman spectroscopy together with XPS caracterization allows inferring the presence of "polyaniline-like" segments formed from *para* coupling during polymerization and also "phenazine-like" segments from *ortho* coupling leading to a ladder structure.

Introduction

Polymer-modified electrodes have been the subject of a wide range of studies, and they have received a great deal of attention owing to their interesting physicochemical properties.[1] These properties made them suitable for applications in batteries, sensors, electrochromic devices, corrosion protection, etc.[2] Oyama et al.[3] have shown that monomers containing $-NH_2$ or $-OH$ as functional groups are suitable candidates for polymerization, leading to very interesting materials that, in some cases, formed double-stranded ladder structures, for example, *o*-phenylenediamine[4,5] or *o*-aminophenol.[6−8]

Poly(5-amino-1-naphthol) (poly(5-NH_2-1-NAP)) is a polymer that belongs to the conducting polymer class obtained by the oxidation of a bifunctional monomer, in this case, 5-amino-1-naphthol. Depending on the electrolytic media, this monomer can be polymerized giving different materials. In organic and acid electrolytes, polymerization takes place via the amino groups, and in basic medium, $-OH$ groups react and lead to the formation of a poly(naphthalene oxide) structure. Poly(5-amino-1-naphthol) is formed in acid media, and it was already demonstrated by using the XPS technique[9] that the $-OH$ group is unaffected during polymerization. The electrochemical behavior of these films has been extensively studied in organic and aqueous media by some "in situ" techniques such as probe beam deflection (PBD) and multiple internal reflection Fourier transform infrared spectroscopy (MIRTFTIRS).[10] A "polyaniline-like" structure (Scheme 1) was proposed as the polymerization product, the redox behavior following the formation of polarons and bipolarons. Mostefai et al.[11] have shown that, during the redox process, the amine group is reversibly transformed in imine. In aqueous acid media, protons play the main role in the charge compensation process in the polymer matrix. The deprotoned salt loses two electrons, leading to the formation of a radical cation, electronic relaxation, and delocalization producing a semiquinoid character.[10,11]

Scheme 1

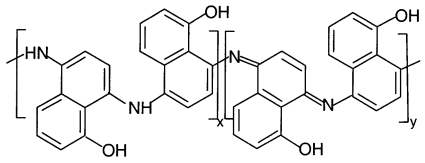

Scheme 2

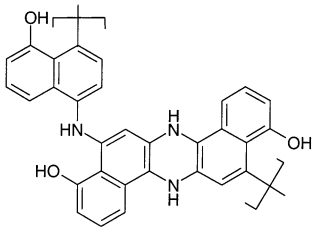

Most spectroscopic studies found in the literature on this material were carried on by using different infrared experimental setups, but not much information was obtained with Raman spectroscopy. Recently, Cintra et al.[12] have presented preliminary resonant Raman results, and the coexistence of two structural forms in the polymeric matrix was proposed: a "polyaniline-like" structure mentioned before that must be formed by majority *para* coupling of the amine group and another, resulting from *ortho* coupling, with a "ladderlike" structure containing nitrogen heterocycles as shown in Scheme 2.

The present paper presents new evidence of the formation of this structure in some parts of the polymeric chains by a complete resonant Raman study combined with XPS characterization.

* To whom correspondence should be addressed: e-mail storresi@iq.usp.br; phone +55 11 309 12165, Fax +55 11 38155579.

10.1021/ma025811x CCC: $25.00
Published on Web 02/15/2003

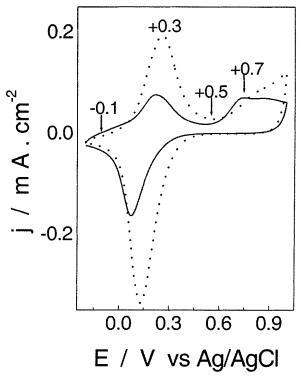

Figure 1. *j*/*E* potentiodynamic profiles of poly(5-NH_2-1-NAP) films grown from a 5-amino-1-naphthol (1×10^{-3} mol L^{-1}) + acid media electrolytic solutions (• • •) HCl 1 mol L^{-1} and (—) HCSA 1 mol L^{-1}. Both films were cycled in the same acid used for polymerization. $V = 0.01$ V s^{-1}.

Experimental Section

Reagents. The monomer 5-NH_2-1-NAP was sublimed under reduced pressure for purification. All acid solutions were prepared from analytical grade chemicals HCl (Merck) or camphorsulfonic acid (Aldrich) and purified water (Millipore system). The latter reagent was purified by recrystallization with ethyl acetate for "in situ" Raman experiments.

Electrochemical Synthesis. Poly(5-NH_2-1-NAP) films were electropolymerized gold (1.0×1.3 cm) plates by applying triangular potential sweeps (0.05 V s^{-1}) in the 0.0−0.9 V (first and second cycles) and 0.0−0.7 V (subsequent cycles) potential ranges. All potentials are referred to the Ag/AgCl electrode, and a platinum wire was used as counter electrode. The polymerization was carried out in a 1×10^{-3} mol L^{-1} monomer + 1 mol L^{-1} acid (HCl or camphorsulfonic acid(HCSA)) electrolytic solution. The use of less positive potentials from the third cycle onward prevents the formation of overoxidized units. After polymerization films were carefully rinsed with purified water and placed in an electrochemical cell containing a free monomer acid electrolytic solution. All experiments were carried out with a EG&G PAR 273 potentiostat/galvanostat.

Spectroscopy. FT-Raman experiments ($\lambda_0 = 1064$ nm) were performed with a FT Raman spectrometer from Bruker (model RFS100). The laser power was kept at 150 mW for "in situ" and 25 mW for "ex situ" experiments. Raman experiments in the visible region ($\lambda_0 = 457.9$, 514.5, and 647.1 nm) were performed with a multichannel Jobin Yvon spectrometer (model T64000) containing a metallurgical microscope and a CCD detector. All experiments were performed with the same microscope objective (50×).

X-ray Photoelectron Spectroscopy (XPS). All experiments were carried out in a Leybold LHS 12 spectrometer by using the Mg Kα source at 12 kV and 10 mA in a vacuum chamber at 8×10^{-5} Torr. The fitting of the curves was made by the Gaussian addition method, and the parameters were maintained constant for all the analysis. In this case all films were deposited onto gold substrates, and more experimental details about sample preparation will be described later.

Results and Discussion

Figure 1 shows the *j*/*E* potentiodynamic behavior of films of poly(5-NH_2-1-NAP) polymerized and cycled in HCl and HCSA electrolytic solutions. It was already discussed in a previous publication[12] that the potential and the intensity of the current peaks are highly dependent on the chemical nature of the electrolytic media. There is a deep loss of electroactivity in the presence of big organic anions such as HCSA. It can be clearly observed a first quasi-reversible redox couple with the oxidation peak at ca. 0.3 V and the reduction peak at −0.25 V. When the potential is increased, another anodic peak appears at ca. +0.7 V, but no reduction peak is observed. For long and reproducible cycling, the potential range must be kept until +0.5 V to avoid the latter irreversible process. Arrows depicted in the picture show the potentials where "in situ" Raman spectra were performed.

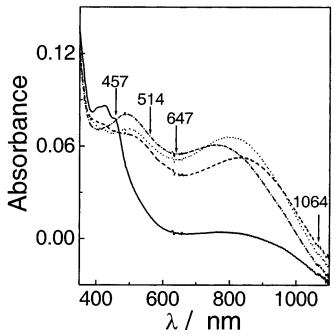

Figure 2. "In situ" visible absorption spectra of poly(5-NH_2-1-NAP) deposited onto ITO electrode, polymerized, and cycled in HCl: (—) −0.2 V, (- - -) +0.3 V, (• • •) +0.5 V, and (- • -) +0.7 V.

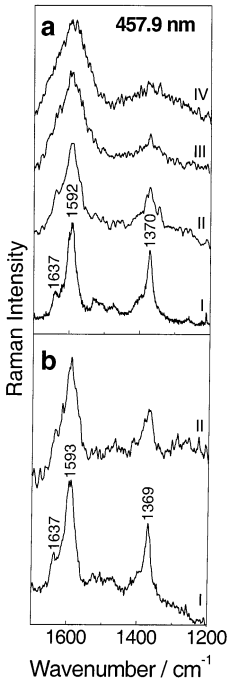

Figure 3. "In situ" resonance Raman spectra ($\lambda_0 = 457.9$ nm) of poly(5-NH_2-1-NAP) electropolymerized in HCl 1 mol L^{-1} and cycled in (a) HCl and (b) HCSA. Different applied potentials were (I) −0.10 V, (II) +0.30 V, (III) +0.50 V, and (IV) +0.70 V.

Figure 2 shows a set of "in situ" absorption spectra carried out with a film polymerized and cycled in HCl electrolytic solution. The electronic spectra of this material were already described in a previous publication,[12] but the purpose here is to facilitate the discussion of resonant Raman results that will be presented later. The arrows in the picture correspond to the excitation lines used in this work.

Figures 3 and 4 show a set of "in situ" Raman spectra obtained with films cycled in different acids for two excitation lines, $\lambda_0 = 457.9$ nm (blue) and $\lambda_0 = 514.5$ nm (green), respectively. It can be seen that for these two excitation lines there are no great changes in the Raman spectra upon oxidation. Moreover, spectra corresponding to the reduced state are clearly defined with

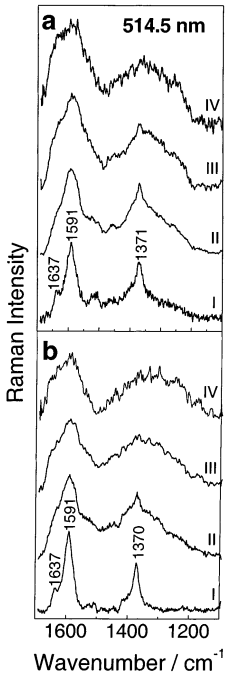

Figure 4. "In situ" resonance Raman spectra ($\lambda_0 = 514.5$ nm) of poly(5-NH_2-1-NAP) electropolymerized in HCl 1 mol L^{-1} and cycled in (a) HCl and (b) HCSA. Different applied potentials were (I) −0.10 V, (II) +0.30 V, (III) +0.50 V, and (IV) +0.70 V.

narrow bands and a higher signal/noise ratio than spectra obtained at higher potentials due to the fact that the oxidized form is out of resonance conditions at these wavelengths. At −0.1 V (reduced state), two important bands can be observed at 1370 and 1590 cm^{-1}. Raising the potential, both bands enlarge due to the growing of other ones that are not well-defined at these excitation lines. Before assigning the bands, Raman and infrared spectra of the monomer and naphthalene were performed, and all vibrational modes were assigned. Table 1 summarizes all the information and assignments for comparison. The band at 1370 cm^{-1} was already attributed[13−15,17] to C−C stretching, which is reliable considering that naphthalene and the monomer present an intense band in the same position, but some controversy remains. Other authors have attributed this band to the combination of (νC−C) and (νC−O)[18] or (νC−C) and (νC−N)[9] or also to the (βC−H).[19] The band at 1590 cm^{-1} is assigned to the stretching (νC−C)[9,13,14,19] of the aromatic rings, and upon oxidation, this band enlarges and forms a shoulder at ca. 1620 cm^{-1}. Simultaneously, a loss of intensity and definition of the band at 1370 cm^{-1} is observed, showing that this band is related to reduced species while the enlargement of the 1590 cm^{-1} band to oxidized ones.

The attribution of the small band that appears at ca. 1637 cm^{-1} is the subject of controversy and discussion. Naphthalene and 5-amino-1-naphthol Raman spectra present a band at ca. 1630 cm^{-1} assigned to the stretching (νC−C). Some authors[11,21] working mainly with infrared spectroscopy assigned this band to the (νC═N) mode, that is to say, to oxidized segments. This assignment must be ruled out because, even in the reduced state, the band is present in all films studied, showing that it must be related to some species or structure formed during polymerization. In a previous publication,[12] we have proposed the assignment of this band as being related to nitrogen-containing heterocyclic rings resulting form *ortho* coupling during polymerization, leading to segments as those shown in Scheme 2.

Figure 5 shows the Raman spectra of films polymerized in HCl or HCSA and cycled in these electrolytic media taken with the red excitation line ($\lambda_0 = 647.1$ nm). This radiation enhances the bands corresponding to the oxidized segments due to the resonant effect. Even in this radiation, in all the films studied, at the reduced state, the main bands that appeared in the Raman spectra are those at 1370 and 1590 cm^{-1} which have already been described. In contrast with results obtained with the blue or the green lines, spectra obtained at this radiation present a better signal/noise ratio, and other small bands are defined at this potential. Upon oxidation, well-resolved Raman spectra are obtained for all films, and some bands are observed at ca. 1260 cm^{-1} and in the 1300−1350 cm^{-1} region. The former one is observed at 1264 cm^{-1} for films cycled in HCl (Figure 5a,b) and at 1258 cm^{-1} in films cycled in HCSA (Figure 5c,d). It was attributed to the (νC−N) mode for polyaniline,[23] and it is apparently influenced by the chemical nature of the electrolyte. Some authors[23−25] have attributed the bands in the 1300−1350 cm^{-1} region to semioxidized charged nitrogen species, of the type $C-N^{\bullet+}$, being better resolved in the spectra corresponding to films polymerized in HCl (Figure 5a,c) than in films formed in HCSA (Figure 5b,d). On the other hand, film oxidation produces also the growth of three bands in the 1450−1550 cm^{-1} region at 1455, 1502, and 1523 cm^{-1}. These bands can be assigned to the stretching of (νC═C) and (νC═N) modes, but it is difficult to do a true assignment. Both the monomer 5-NH_2-1-NAP and naphthalene present a band at 1448 and 1458 cm^{-1}, respectively; that is why the band at 1455 cm^{-1} should be assigned to the νC−C mode. The bipolaronic form of polyaniline presents a band at 1485 cm^{-1} well discussed in the literature[26] and already assigned to the νC═N mode and another at 1515 cm^{-1} attributed to the bending of N−H bond.[23,24] It can be seen that for more electroactive films, electropolymerized in HCl (Figure 5a,c), the relative intensity of the band located at 1502 cm^{-1} is greater than that of the band at 1523 cm^{-1} when the film is polarized at more positive potentials. This is evidence that this band can be attributed to imine groups formed at high dopage levels. At higher frequencies, in the 1600 cm^{-1} region, as the potential is raised, the band at 1589 cm^{-1} enlarges and a shoulder is formed at 1573 cm^{-1}. These bands are assigned to the aromatic and quinoid form, respectively, of the aromatic rings. At ca. 1640 cm^{-1} the small band already described is also present in the different films, and it is evident that, in some cases (Figure 5a,c), its relative intensity increases as the potential is raised. This band have been already observed by other authors, and it was assigned to the ring breathing mode of heterocyclic segments containing nitrogen atoms.[27,28]

The set of Raman spectra shown in Figure 6 was obtained in another point of the same sample than those shown in Figure 5. It is important to point out that, as the experimental setup used here was the micro-Raman mode, it is possible to obtain spectra at different points in the same sample with a spatial resolution of ca. 2.0 μm^2. As can be seen in the figure, even the spectra obtained at −0.1 V were the same as those in Figure 5; the evolution of the Raman spectra when films were oxidized is completely different. In these cases, spectra obtained at 0.5 and 0.7 V have an excellent signal/noise

Table 1. Observed Frequencies (in cm^{-1}) of 5-NH_2-1-NAP and Naphthalene in Raman Spectra at Different Excitation Lines[a]

5-NH_2-1-NAP 457 nm	5-NH_2-1-NAP 647 nm	5-NH_2 1-NAP 1064 nm	naphthalene 1064 nm	probable mode of vibration
512 (m)	511 (m)	511 (w)	513 (s)	α(CCC)[14]
660 (s)	660 (s)	661 (s)		α(CCC)[14]
				ring breathing ν(CC)[13]
754 (m)		754 (w)		γ(CH)[13]
				ring breathing ν(CC)[13,14]
			764 (s)	γ(CH)[13]
863 (m)	860 (w)	862 (m)		β(CH)[13]
957 (vw)	959 (vw)	960 (vw)		γ(CH)[13,14]
			1022 (w)	ν(CC)[14]
1057 (vw)	1054 (vw)	1056 (w)		
			1147 (w)	β(CH),[14] ring deformation[15]
			1171 (vw)	β (CH)[14]
			1243 (vw)	β (CH)[14]
1262 (w)	1259 (w)	1260 (w)		ν (CN)[16]
1386 (vs)	1383 (vs)	1383 (vs)	1380 (vs)	ν (CC),[13−15,17] ν (CC) +ν (CO)[18]
1448 (w)	1444 (w)	1446 (w)	1444 (w)	ν (CC)[13,14,18]
			1463 (w)	ν (CC),[13,18] β (CC)[14]
1582 (m)	1580 (m)	1583 (m)	1577 (m)	ν (CC)[9,13−15,20]
1627 (w)		1628 (vw)	1628 (w)	ν (CC)[13,18]
3009 (s)	3013 (s)	3008 (m)	3007	ν (CH)[13,16]
3060 (m)	3063 (m)	3059 (m)	3056 (m)	ν(CH)[16−18]
3077 (s)	3080 (s)	3077 (s)	3085 (s)	ν(CH)[17]
3298 (w)	3302 (w)			ν(NH)[16,20]
3386 (m)	3388 (m)			ν(NH)[16,20]

[a] Key: vs = very strong, s = strong, m = medium, w = weak, vw = very weak.

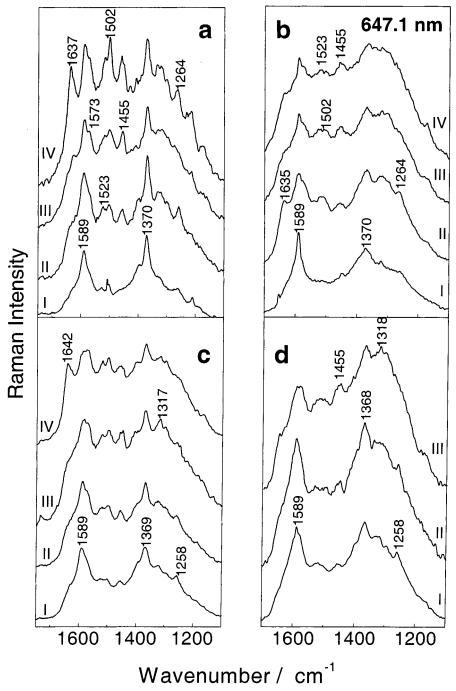

Figure 5. "In situ" resonance Raman spectra ($\lambda = 647.1$ nm) of poly(5-NH_2-1-NAP) at different potentials. (a) film electropolymerized and cycled in HCl; (b) electropolymerized in HCSA and cycled in HCl; (c) film electropolymerized in HCl and cycled in HCSA; (d) electropolymerized and cycled in HCSA. Different applied potentials were (I) −0.10 V, (II) +0.30 V, (III) +0.50 V, and (IV) +0.70 V.

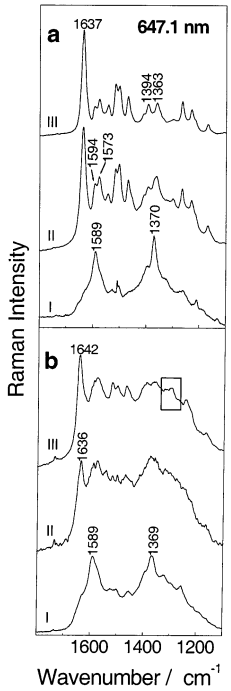

Figure 6. "In situ" resonance Raman spectra ($\lambda_0 = 647.1$ nm) of poly(5-NH_2-1-NAP) electropolymerized in HCl 1 mol L^{-1} and cycled in (a) HCl and (b) HCSA. Data obtained in different points than those shown in Figure 5a,c. Different applied potentials were (I) −0.10 V, (II) +0.50 V, and (III) +0.70 V.

ratio and some new bands appear. The band at 1370 cm^{-1} disappears upon oxidation while two new bands grow at 1363 and 1394 cm^{-1}, and bands in the 1400−1550 cm^{-1} region are shift to higher frequencies. The shoulder observed at 1573 cm^{-1} and assigned to the ν(C=C) of the quinoid rings (Figure 5) is now a well-resolved band with its relative intensity higher than that of the band at 1589 cm^{-1}, which is now shifted to 1594 cm^{-1}. But the most remarkable fact in these set of spectra is the raise of intensity of the band located at 1640 cm^{-1}. In the film polymerized and cycled in HCl (Figure 7a) it is possible to observed that, simultaneously with the raise of the 1640 cm^{-1} band at high positive potentials, there is the diminution of the bands of the 1300−1350 cm^{-1} region corresponding to the semioxidized species $C-N^{\bullet+}$. This behavior is observed for all the other films (Figure 6b) but to a lower extent than in Figure 6a. This is evidence that the oxidation is not so effective when films are polymerized or cycled

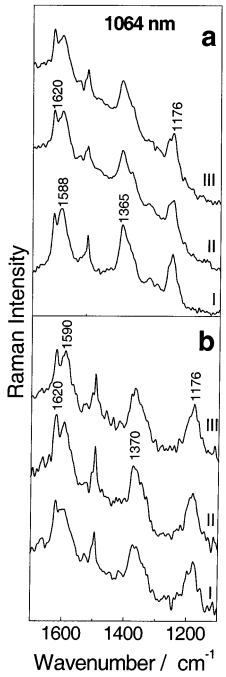

Figure 7. "In situ" resonance Raman spectra ($\lambda_0 = 1064$ nm) of poly(5-NH_2-1-NAP) electropolymerized in HCl 1 mol L^{-1} and cycled in (a) HCl and (b) HCSA. Different applied potentials were (I) −0.10 V, (II) +0.30 V, and (III) +0.70 V.

in HCSA, which is in agreement with its lower electroactivity observed in electrochemical experiments. At this point, it is important to remark that this behavior was found in specific points of the samples, and the evolution of Raman spectra is reversible; that is to say, if a reduction potential is applied, the original spectrum is recovered. These experiments show that polymerization occurs, producing a nonhomogeneous material where different segments coexist and take part in the redox processes of the polymer. On the other hand, the chemical nature of the electrolyte plays a very important role in the charge stabilization process in the different polymeric segments.

Figure 7 shows the Raman spectra obtained with different films in HCl and HCSA electrolytic media at $\lambda_0 = 1064$ nm. It is important to point out that the system is out of resonance conditions at this wavelength, as it can be seen in Figure 2. In a different way than the behavior observed with other excitation radiation, not many changes are observed by increasing the potential. Anyway, this is a very important result because, as no changes are observed upon oxidation in this out of resonance condition, this is evidence that the dopage level is low at this material in agreement with Oyama et al.,[3] who reported a conductivity of ca. 10^{-6}−10^{-7} S cm^{-1} for this doped polymer in the dried state. At this radiation, it is possible to observe the increase of the bands at 1176 and 1620 cm^{-1}. The former one is related to the in-plane bending of the C−H bond, and the latter is assigned to the (νC−C) of the ring.[14]

The XPS technique was used in a complementary way to resonant Raman studies. As the area analyzed in XPS experiments is much greater than in micro-Raman studies, it must be pointed out that information in this case will be an average composition of the surface. That is why micro-Raman experiments were performed at different points of the sample in order to map the surface and to correlate data obtained by both different techniques. Figure 8 shows the extended spectra of poly-

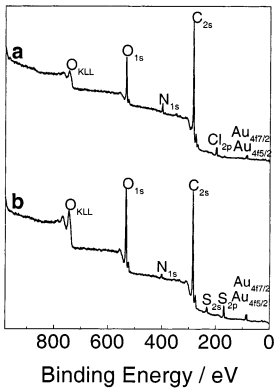

Figure 8. XPS wide scan of poly(5-NH_2-1-NAP) films (a) electropolymerized and cycled in HCl and (b) electropolymerized and cycled in HCSA.

(5NH_2-1-NAP) formed in either HCl or HCSA media. Pham et al.[9] have already studied this polymer by XPS focusing on C and O bands in order to determine that no oxidation of the −OH group takes place. In this paper all attention was paid to the nitrogen atom in order to obtain information about the different segments that can be present in the polymeric chains. As can be seen in Figure 8, the analysis of the data must be carefully done due to the low intensity of the nitrogen band. All films were prepared by electrochemical cycling onto gold electrodes. After polymerization, films were rinsed with distilled water in order to remove monomer or electrolyte traces. Films were put in an electrochemical cell with a free monomer solution with the same acid used in the polymerization process (HCl or HCSA). A potential of −0.2 V was applied, and the current was recorded until a constant value was reached. After this procedure, electrodes were washed with water and placed for 20 min in a desiccator flask to dry and then placed in the XPS vacuum camber. Two other films followed the same experimental procedure, but they were polarized at +0.5 V until a constant current was reached. After that, films were washed with distilled water and dipped in a NaOH 2 mol L^{-1} solution to obtain the deprotonated state, rinsed again, and put to dry before placing them in the XPS vacuum chamber.

Figure 9 shows the N 1s spectra and the fitting curves calculated to identify the different contributions for films polymerized and cycled in HCl or HCSA in both the reduced and the oxidized states. For a better understanding, the corresponding calculated percent area of each peak is depicted in Table 2. As can be seen in the figure, for both films studied here, while the energy value of each peak was the same, the percent area varied depending on the oxidation state of the sample. In the reduced state, the predominant species is obviously amine (−NH−) giving a value of 74% in HCl and 58% in HCSA, while the imine (=N−) percent is almost the same in both cases; on the contrary, the amount of charged nitrogens (N^+) is largely greater in HCSA than in HCl. The explanation of this phenomenon is related to the fact that HCSA is less volatile than HCl, so that, even after being in the vacuum chamber, HCSA continues at the sample surface leading to the increase of charged species N^+.[29] When a potential of +0.5 V is applied, it can be seen that the sample is in the semioxidized form, and a large amount of nitrogen atoms remains in the amine state (39% and 43% for HCl and HCSA, respectively) while the amount of imine (=N−) species has been increased. Special attention

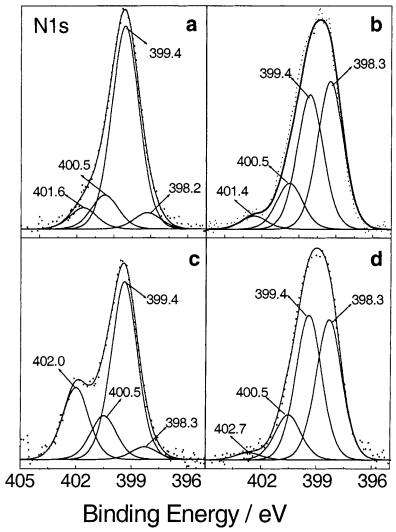

Figure 9. XPS N 1s narrow scan of poly(5-NH_2-1-NAP) films: prepared and treated in HCl in (a) reduced state and (b**)** oxidized state; prepared and treated in HCSA in (c) reduced state and (d) oxidized state. Raw data (· · ·) were fitted (—) by using the Gaussian addition method.

Table 2. N 1s Data of Poly(5-NH_2-1-NAP) from XPS Results

N 1s binding energy (eV)	HCl proportion (%)		HCSA proportion (%)	
	RED	OXID	RED	OXID
398.2	5.9	43.3	4.1	41.6
399.4	73.9	39.4	58.0	42.9
400.5	12.4	13.5	14.3	13.3
401.6	7.8	3.9		
402.1			23.5	2.1

must be put in the analysis of the fourth peak resulting from the fitting process and located at 400.5 eV. Some authors[30,31] have assigned this peak to one of the possible forms of charged nitrogen (−N^+−) and other authors[33] to the presence of heterocyclic nitrogens. As can be seen, this peak appears in both the reduced acid state and the oxidized basic one. Another striking fact is that the percent area of the peak does not change with the oxidation state. The assignment of this peak to protonated species must be ruled out because, even after dipping the electrode in NaOH solutions, it remains with the same intensity. This result is another evidence of the presence of a "ladder" structure resulting from *ortho* coupling during polymerization, coexisting with a "polyaniline-like" structure in the polymeric matrix.

Conclusions

Resonant Raman spectroscopy allowed to characterize all structures that are formed upon oxidation of poly-(5-NH_2-1-NAP) films in acidic media. The band at ca. 1640 cm^{-1} was attributed to the presence of nitrogen-containing heterocycles formed during polymerization. The use of the micro-Raman mode allowed finding regions with different chemical composition, leading to different Raman patterns upon oxidation. In these regions the enhancement of the band at 1640 cm^{-1} upon oxidation showed that these segments are electroactive with high resonant behavior in the red. X-ray photoelectron spectroscopy in the N 1s edge also confirmed the existence of a certain percent of heterocyclic nitrogens. It is important to point out that the amount of these segments does not depend significantly on the oxidation state of the polymer. The combination of resonant Raman and XP spectroscopy allow to confirm the formation of ladder structure in poly(5-NH_2-1-NAP).

Acknowledgment. Authors thank Brazilian agencies CNPq and FAPESP for financial support. E.P.C. thanks CNPq (572251/1998-0) and CAPES (BEX0045/01-2) for scholarships granted in Brazil and France, respectively. This paper was carried out with the economic support of a USP−COFECUB collaboration.

References and Notes

(1) Maia, D. J.; De Paoli, M.-A.; Alves, O.L.; Zarbin, A. J. G.; Neves, S. *Quim. Nova* **2000**, *23* (*2*), 204−215.
(2) Li, X.-G.; Huang, M.-R.; Duan, W.; Yang, Y.-L. *Chem. Rev.* **2002**, *102*, 2925−3030.
(3) Ohsaka, T.; Ohba, M.; Sato, M.; Oyama, N. *J. Electroanal. Chem.* **1991**, *300*, 51−66.
(4) Malinauskas, A.; Bron, M.; Holze, R. *Synth. Met.* **1998**, *92*, 127−137.
(5) Wu, L.-L.; Luo, J.; Lin, Z.-H. *J. Electroanal. Chem.* **1996**, *417*, 53−58.
(6) Barbero, C.; Silber, J. J.; Leonides, S. *J. Electroanal. Chem.* **1989**, *263*, 333−352.
(7) Jackowska, K.; Bukowska, J.; Kudelski, A. *J. Electroanal. Chem.* **1993**, *350*, 177−187.
(8) Kunimura, S.; Ohsaka, T.; Oyama, N. *Macromolecules* **1988**, *21*, 894−900.
(9) Pham, M.-C.; Mostefai, M.; Simon, M.; Lacaze, P.-C. *Synth. Met.* **1994**, *63*, 7−15.
(10) Barbero, C.; Haas, O.; Mostefai, M.; Pham, M.-C. *J. Electrochem. Soc.* **1995**, *142*, 1829−1833.
(11) Mostefai, M.; Pham, M.-C.; Marsault, J.-P.; Aubard, J.; Lacaze, P.-C. *J. Electrochem. Soc.* **1996**, *143*, 2116−2119.
(12) Cintra, E. P.; Córdoba de Torresi, S. I. *J. Electroanal. Chem.* **2002**, *518*, 33−40.
(13) Singh, R. D.; Sharma, O. P.; Bhatti, H. S.; Nair, N. V. U. *Indian J. Pure Appl. Phys.* **1982**, *20*, 635−641.
(14) Michaelian, K. H.; Ziegler, S. M. *Appl. Spectrosc.* **1973**, *27*, 13−21.
(15) Shinohara, H.; Yamakita, Y.; Ohno, K. *J. Mol. Struct.* **1998**, *442*, 221−234.
(16) Akalin, E.; Akyuz, S. *Vib. Spectrosc.* **2000**, *22*, 3−10.
(17) Sellers, H.; Pulay, P.; Boggs, J. E. *J. Am. Chem. Soc.* **1985**, *107*, 6487−6494.
(18) Nogueira, H. I. S.; Quintal, S. M. O. *Spectrochim. Acta, Part A* **2000**, *56*, 959−964.
(19) Menendez, J. R.; Obuchowska, A.; Aroca, R. *Spectrochim. Acta, Part A* **1996**, *52*, 329−336.
(20) Lin-Vien, D. In *The Handbook of Infrared and Raman Characteristc Frequencies of Organic Molecules*; Colthup, N. B., Fateley, W. G., Grasselli, J. G., Eds.; Academic Press: Boston, 1991; p 161.
(21) Meneguzzi, A.; Ferreira, C. A.; Pham, M.-C.; Delamar, M.; Lacaze, P. C. *Electrochim. Acta* **1999**, *44*, 2149−2156.
(22) Boyer, M. I.; Quillard, S.; Rebourt, E.; Louarn, G.; Buisson, J. P.; Monkman, A.; Lefrant, S. *J. Phys. Chem. B* **1998**, *102*, 7382−7392.
(23) Boyer, M. I.; Quillard, S.; Cochet, M.; Louarn, G.; Lefrant, S. *Electrochim. Acta* **1999**, *44*, 1981−1987.
(24) Bernard, M.-C.; Le Goff, A. H. *Synth. Met.* **1997**, *85*, 1145−1146.
(25) Pereira da Silva, J. E.; De Faria, D. L. A.; Córdoba de Torresi, S. I.; Temperini, M. L. A. *Macromolecules* **2000**, *33*, 3077−3083.
(26) Quillard, S.; Berrada, K.; Louarn, G.; Lefrant, S. *New J. Chem.* **1995**, *19*, 365−374.
(27) Lawless, M. K.; Mathies, R. A. *J. Chem. Phys.* **1992**, *96*, 8037−8045.
(28) Vogel, E.; Gbureck, A.; Kiefer, W. *J. Mol. Struct.* **2000**, *550*−*551*, 177−190.
(29) Neoh, K. G.; Pun, M. Y.; Kang, E. T.; Tan, K. L. *Synth. Met.* **1995**, *73*, 209−215.
(30) Fraoua, K.; Delamar, M.; Andrieux, C. P. *J. Electroanal. Chem.* **1996**, *418*, 109−113.
(31) Han, M. G.; Im, S. S. *Polymer* **2000**, *41*, 3253−3262.
(32) Rodrigues, P. C.; Muraro, M.; Garcia, C. M.; Souza, G. P.; Abbate, M.; Schreiner, W. H.; Gomes, M. A. B. *Eur. Polym. J.* **2001**, *37*, 2217−2223.
(33) Rodrigues, D.; Riga, J.; Verbist, J. J. *J. Chim. Phys.* **1992**, *89*, 1209−1214.

MA025811X